5-2022

Small-scale variability in warm season, precipitation around an urban area: a case study of Louisville-Jefferson County, KY.

Isaiah I. Kingsberry
University of Louisville

SMALL-SCALE VARIABILITY IN WARM SEASON, PRECIPITATION AROUND AN URBAN AREA: A CASE STUDY OF LOUISVILLE-JEFFERSON COUNTY, KY

By

Isaiah Kingsberry
B.S. Atmospheric Science, 2018

A thesis
Submitted to the faculty of the
College of Arts and Sciences of the University of Louisville
in partial fulfillment of the requirements
for the degree of

Master of Science in Applied Geography

Department of Geographic & Environmental Sciences
University of Louisville
Louisville, Kentucky

May 2022

SMALL-SCALE VARIABILITY IN WARM SEASON, PRECIPITATION AROUND AN URBAN AREA: A CASE STUDY OF LOUISVILLE-JEFFERSON COUNTY, KY

By

Isaiah Kingsberry

B.S., University of Louisville, 2018

A Thesis Approved on

April 21, 2022

By the following Thesis Committee:

_____

Jason Naylor

Thesis chair

_____

W. Scott Gunter

Committee member

_____

J. Anthony Stallins

Committee member

ACKNOWLEDGMENTS

I would like to send a special thanks to my mentor, Dr. Jason Naylor, for allowing me to be a part of this project and for all the guidance he's extended thus far. I would also like to thank Dr. Andrea Gaughan for her powerful introduction into the world of Geography. To the faculty of the Department of Geographic & Environmental Sciences at the University of Louisville, thank you for providing me not only with an opportunity to continue furthering my education, but for providing me with a cohort of mentorship, too many to thank in this brief volume. The many lessons, both in and out of the textbook will last a lifetime. And finally I would like to thank the National Science Foundation for their financial support which has made this work possible.

ABSTRACT

SMALL-SCALE VARIABILITY IN WARM SEASON, PRECIPITATION AROUND AN URBAN AREA: A CASE STUDY OF LOUISVILLE-JEFFERSON COUNTY, KY

Isaiah I. Kingsberry

April 14, 2022

Numerous studies have detected anomalous precipitation patterns occurring up to 50 km downwind of major cities, providing major evidence that cities inadvertently modify precipitation and atmospheric circulations. Louisville is one such major city with a growing body of evidence of inadvertent precipitation modification. Despite these efforts, the physical mechanisms driving small-scale and unintentional changes in urban precipitation are little understood, being rooted largely in theory rather than in physical observations.

This study seeks to build upon previous research by analyzing ground-based precipitation observations recorded by a high-density gauge network located within approximately 40 km of Louisville's urban center. The results of this research show that precipitation around Louisville, KY have a strong bias for urban enhancement by a median of 14% in all directions. This research also shows a strong bias for directional dependency in the relationship between wind flow and precipitation modification. By improving our understanding of urban precipitation modification, we also improve our ability to predict and effectively mitigate severe weather, especially those events which threaten dense and vulnerable population centers.

TABLE OF CONTENTS

ACKNOWLEDGMENTS iii

ABSTRACT iv

LIST OF FIGURES viii

INTRODUCTION 1

DATA 6

STUDY AREA 6

MSD RAIN GAUGE DATA 8

NOAA NEXT GENERATION RADAR (NEXRAD) LEVEL II BASE DATA 9

NCEP-DOE AMIP-II REANALYSIS (R-2) 10

SPATIAL SYNOPTIC CLASSIFICATION 10

METHODS 11

GAUGE VERIFICATION 11

CALCULATION OF 0-6 KM MEAN WINDS 15

DOWNWIND AND UPWIND COMPARISON 15

RESULTS 18

GAUGE PERFORMANCE ANALYSIS 18

WARM SEASON, SHORT TERM CLIMATOLOGY (2017-2020) 20

DOWNWIND TO UPWIND ANALYSIS 22

BY SYNOPTIC CLASSIFICATION 23

CONCLUSIONS.....27

REFERENCES 30

CURRICULUM VITA 34

LIST OF FIGURES

Figure 1 – Debbage and Sheppard (2015) Urban heat island and land use land cover analysis of Louisville-MSA 7

Figure 2 – MSD rain gauge network overview in Louisville-Jefferson County, KY 9

Figure 3 – MSD rain gauge network performance analysis results 19

Figure 4 – Histogram of warm seasonal 0–6 km mean wind bearings 20

Figure 5 – Warm seasonal precipitation 2017–2020 (inches/year) 21

Figure 6 – Ordinal directional subsets of (left) total precipitation normalized by mean upwind precipitation and (right) % variance from subset mean precipitation 25

Figure 7 – Histogram of the results of permutations of seasonal median downwind to upwind precipitation amounts and the observed median ratio 26

INTRODUCTION

Developed areas make up less than 6% of land cover in the contingent United States (NLCD 2019). However, they are home to 82% of the United States' population with current projections estimating that as much as 89% of the U.S. population could be living within urban areas by 2050 (UN 2018). The high concentrations of people found within urban areas makes them particularly vulnerable to hazards and disruptions created by severe weather and other natural disasters. The risk of severe weather hazards are further exacerbated by the amount of impervious surface cover incorporated into urban design, which is known to decrease the natural ability of the land to mitigate severe weather, creating additional threats such as severe flash flooding (Feng et al. 2021). As cities continue to expand rapidly across the globe, it is crucial to be able to accurately predict and mitigate severe weather at small scales. However, a growing body of research shows that the very urban centers we aim to protect, are inadvertently driving changes local and mesoscale changes in precipitation.

Numerous studies have shown that highly developed urban areas inadvertently impact precipitation patterns (Changnon 1976; Bornstein and Lin 2000; Diem and Brown 2003; Shepherd and Burian 2003; Shepherd 2005; Naylor 2018). From the intense heat of large expanses of concrete, to the surface roughness created by urban canopies, and even aerosols from urban and industrial activities, cities play an active role in shaping our physical environment. Intensive land use land cover change can greatly modify land-air interactions,

particularly within the boundary layer, leading to patterns of precipitation that may vary greatly from surrounding rural areas.

In their study on eight urban cities, Huff and Changnon (1973) studied historical rain gauge observations utilizing gauge networks that extended between 80–120 km from urban centers. They observed a 9–17% enhancement in precipitation between 15–55 km downwind of six of eight urban areas. In addition, they also found a significant increase in lightning (13–47%) and hail (0–430%) downwind of cities indicating the presence of increased downwind convective activity. The enhancement was found to be especially prevalent during warm season, suggesting the presence of an urban modification effect. Enhancement was seasonal with the strongest in detected in summertime precipitation events with up to a 17% increase in precipitation.

Shepherd et al. (2002) also observed precipitation enhancement downwind of five urban cities using the observations made by the Tropical Rainfall Measuring Mission platform (TRMM). TRMM is a multisensor remote sensing platform designed to monitor and record precipitation at tropical latitudes (NASA 2020). Outfitted with a precipitation radar, visible infrared sensor, a microwave sensor, a radiant energy system and a lightning imaging sensor, TRMM utilizes various remotely monitored cloud properties to model precipitation in continuous 0.5 degree by 0.5 degree grids. TRMM benefits greatly from increased spatial resolution compared to surface-based gauge observations which require the implementation and maintenance of dozens of rain gauge devices. In their study, Shepherd found that using remotely sensed data, precipitation amounts between 20–60 km downwind of urban areas were enhanced by as much as 48%–116% of the mean precipitation amount observed upwind of urban centers. While this is a much greater increase than observed in previous studies,

downwind enhancement could still be observed when modeling precipitation based on remote cloud observations.

More recent efforts have continued to build on previous work through the implementation of more complex investigations while increasing the catalogue of unique. Naylor (2020) modeled idealized squall lines over a simulated urban area to investigate dynamical changes in convective activity due to urban modification. What they found was that in simulations including urban induced thermal and surface roughness gradients, CAPE intensified while updrafts grew more vigorous and widespread even after passing over the simulated city resulting in storm intensification downstream. Similarly, Lin et al (2021) found that in WRF-chem model simulations, convergence due to turbulence as well as increased aerosols over Kansas City caused severe weather intensification over and downwind of the urban center. Although the model had a bias for overestimating rainfall compared to collected observations, it is still in agreeance with various studies throughout the last few decades.

While there has been growing evidence that urban areas influence precipitation patterns, the precise mechanisms through which inadvertent modification occurs are still being investigated. Current theorized modification mechanisms include: destabilizing urban boundary layer perturbations (Orchs and Semonin 1979; Shepherd and Burian 2003); urban aerosols (Diem and Brown 2003; Mölders and Olson 2004); convergence due to surface roughness (Bornstein and Lin 2000; Thielen et al. 2000); and system diversion by urban canopy (Loose and Bornstein 1977; Bornstein and Lin 2000). These mechanisms focus largely on the modification of boundary layer properties over urban areas leading to a stark contrast with surrounding rural areas

Intensive land use land cover change dramatically modifies land-air interactions. By replacing vegetative and natural land cover with built land cover we greatly change the thermal characteristics of land cover. Compared to cities, continuously vegetative land covers have high surface albedo. This leads to more reflection of incoming solar radiation in rural areas and greater warming of the lower atmosphere in urban environments (Shepherd 2005). Additionally, the lower specific heat of concrete and built surfaces when compared to vegetation leads to more efficient conversion of incoming short-wave radiation to outgoing long-wave radiation in urban environments. These differences in the thermal properties of urban and rural environments results in increased heating in urban environment compared to surrounding rural areas. As heating in the boundary layer is largely driven by outgoing long-wave radiation by the surface, air temperature gradients develop which can influence local patterns of precipitation. Similarly, both the urban heat island and surface roughness spurred on by intensive LULC change can cause an increase in localized turbulence. This increased air turbulence can lead to convergence over urban centers leading to the intensification of storms over cities and downwind.

Urban generated aerosols may also lead to storm modification. Depending on the quantity and composition of aerosols, they have been shown to either enhance or suppress cloud droplet growth and thus rainfall (Rosenfeld 2000). In cases of enhancement, aerosols may act as cloud condensation nuclei, making it easier for droplets to grow beyond their critical radius and thus enhancing the potential for precipitation. Conversely, aerosols which are hydrophobic may interfere with droplet growth, suppressing precipitation. Aerosols may also enhance the urban heat island effect, creating additional convergence and enhanced precipitation.

While previous studies focused on precipitation patterns across large areas or else relying on modeled data, this study will focus on a high-density network contained within 40 km of an urban center. A high-density rain gauge network provides enhanced spatial resolution that better reflects the spatial complexity and variability found in an urban environment. A high-density gauge network is also uniquely situated to compete with the spatial resolution provided by remotely sensed and modeled precipitation products while providing the certainty of direct sensed precipitation. By also including storm motion, this study will be able to investigate rainfall enhancement downwind of urban centers while capturing the spatial complexity across a discontinuous and sprawled urban environment. End results will be able to deduce if urban modification can be detected within the immediate vicinity of a major urban center.

This study will be investigating several hypotheses. The first hypothesis is that there is detectable enhancement downwind of Louisville, KY during the warm season, defined hereon as the months of March through October. By comparing regions immediately upwind and downwind of the city's center the relevance and magnitude of precipitation enhancement may be determined. Secondly, is that the magnitude of precipitation enhancement is dependent on environmental, synoptic and mesoscale conditions, in this case air mass classification and convective strength as indicated by reflectivity. This research will prepare future work into the machinations of urban precipitation enhancement by providing a framework and determining the effectiveness of using a publicly available, dense rain gauge network for research in urban modification.

DATA

STUDY AREA - LOUISVILLE-JEFFERSON COUNTY, KY

Louisville-Jefferson County, KY is a consolidated county-city and Kentucky's largest city. The consolidation of Louisville and Jefferson County into one government occurred in 2003 making Louisville the largest city in Kentucky. This consolidation however has resulted in a sprawled pattern of development across the county as many smaller cities were also merged with Louisville Metro. The sprawled, urbanization found in Louisville Metro uniquely situates the county-city for investigations into urban modification within and immediately surrounding an urban area. Additionally, Louisville is home to a dense rain gauge network and Doppler weather radar, KLVX which make it a desirable location to study urban precipitation

As early as 1961, Louisville, KY has become well known for its urban heat island effect (Demarris 1961). The county-city's sprawl style development has led to widespread and discontinuous development, characterized by intensive land clearance and expanses of developed land cover, despite its relatively low population. Since the discovery of its urban heat island, Louisville has been involved in notable urban heat island investigations (Stone 2007; Debbage and Sheppard 2015). In several of such studies, Louisville, KY was found to host one of the largest urban heat islands in the United States (Mattson et al. 1978; Debbage and Sheppard 2015), boasting as large as a 6.5 degrees Celsius temperature difference between Louisville and surrounding rural areas.

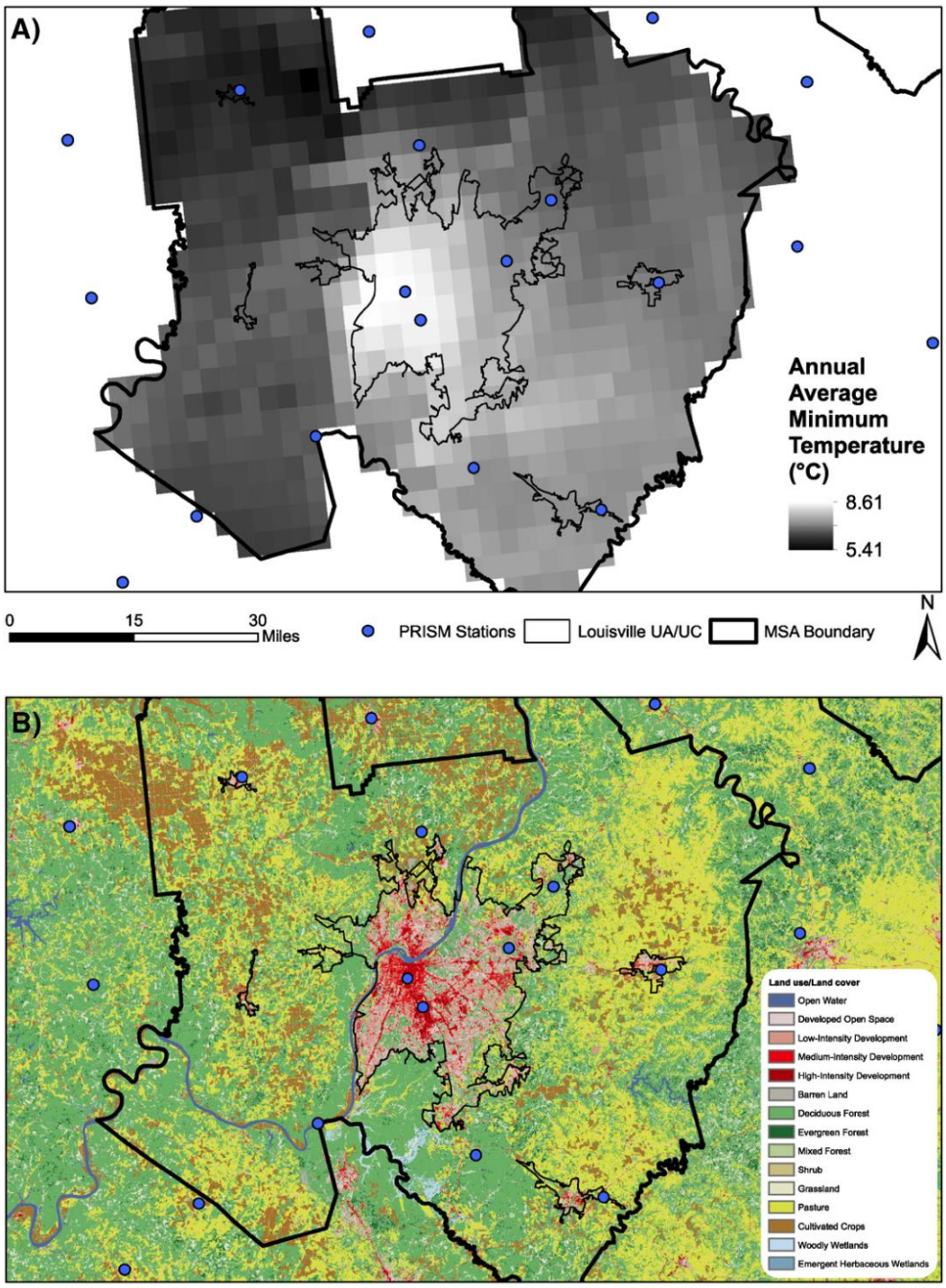

Figure 1. Urban heat island analysis of Louisville-MSA performed by Debbage and Sheppard (2015) depicting: A) 2010 gridded, PRISM annual average minimum surface temperature; B) 2006 National Land Cover Database classification.

MSD RAIN GAUGE DATA

Gauge observations were obtained from a publicly available dataset maintained and provided by Louisville-Jefferson County Metropolitan Sewage District (MSD 2021). The rain gauge network contains 46 gauges within and surrounding Jefferson County, KY (figure 2). 29 gauges provided high spatial coverage within Jefferson County while the rest provided limited coverage in 7 surrounding counties including 3 Indiana counties. In total, the network covers approximately 2,000 Km^2, roughly twice the area of the city boundaries with gauges concentrated and centered on municipal boundaries.

Data from the gauge network provides direct observations of precipitation, providing reliable measurements of local precipitation. Louisville MSD's network is particularly dense, offering good spatial resolution, approximately 56 square km per rain gauge. Gauge observations are available from 2003. However, the network continued to expand throughout 2018. Therefore, to maximize network spatial and temporal coverage, data from the years 2017 to 2020 will be the research's focus. During this time approximately 40 gauges are active. Maintenance records are not available for the network. To verify gauges' operational status further, gauge accuracy was determined by verifying gauge data with radar observations. Gauges with a tendency to report precipitation without verifiable radar observations were removed from the study leaving 35 operational gauges to maximize spatial and temporal resolution and observational accuracy. Because the winter precipitation capabilities of the network are unknown, the studied period has been limited primarily to the warm season, March through October. By limiting the study to the warm season, the impact of extreme low temperatures and snowfall on gauge performance are avoided.

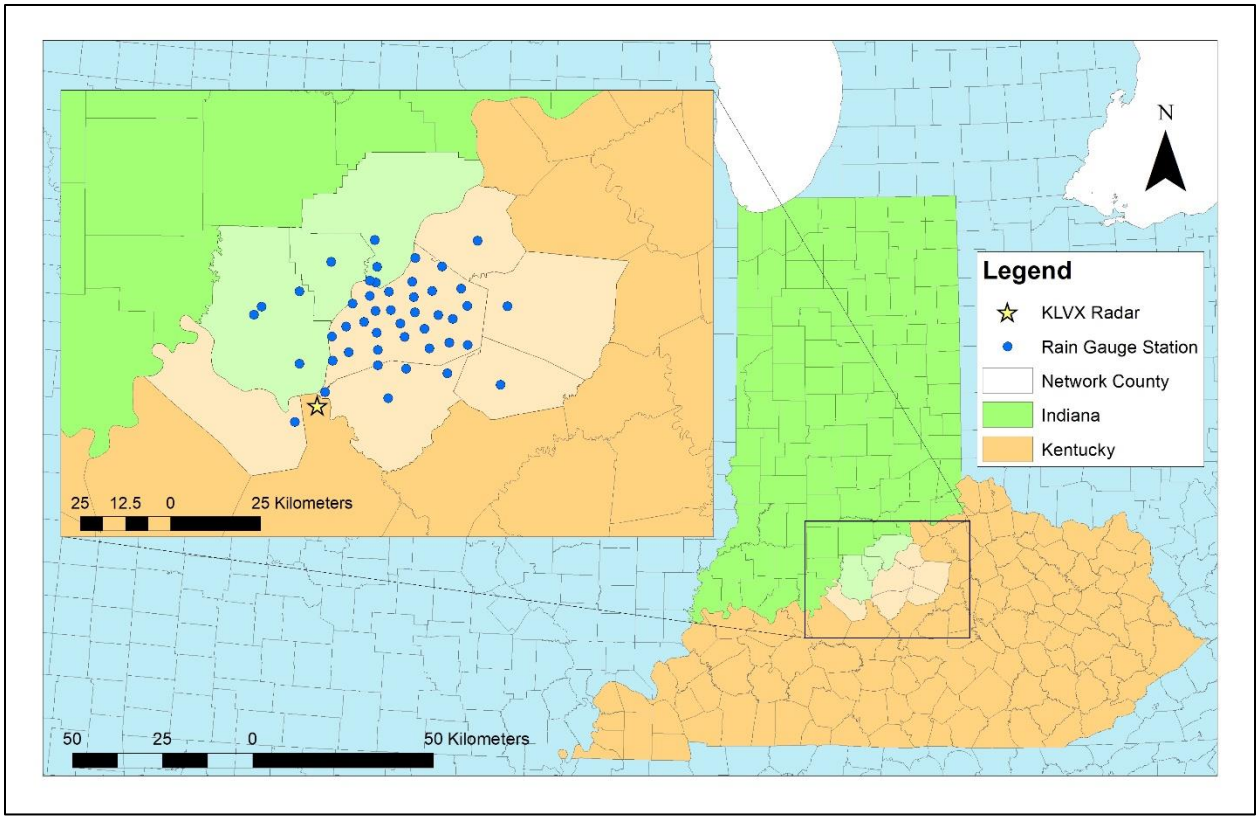

Figure 2. MSD rain gauge network across Louisville-Jefferson County, KY and surrounding counties.

NOAA NEXT GENERATION RADAR (NEXRAD) LEVEL II BASE DATA

The Next Generation Weather Radar (NEXRAD) system is a national radar system of 160 Doppler radars operated by the National Weather System, the Federal Aviation Association, and the U.S. Air Force (NCEI 2021). Radar observations are used in this research to verify the operational status of individual rain gauges throughout the study period. The verification of precipitation requires the investigation of two radar moments: reflectivity; and cross-correlation ratio (CCR). Reflectivity detects the presence and intensity of precipitation by measuring the strength of the return of emitted radio waves. CCR is a product of dual polarization which helps to distinguish between meteorological and non-

meteorological targets through the analysis of their shape. When these two products are interpreted together, they can help to verify the presence of precipitation at gauge locations

NCEP-DOE AMIP-II REANALYSIS (R-2)

NCEP-DOE AMIP-II Reanalysis (R-2) is a multi-source global climate forecasting model that utilizes historic and real-time data from multiple data sources such as: radiosonde; weather station data; aircraft; and satellite observations. R-2 provides global gridded datasets of various climatological parameters available 4 times daily at 2.5 degree by 2.5 degree resolution and 17 pressure levels from 1000 mb to 10 mb. Gridded datasets of U and V wind vector components can be used to approximate daily 0–6 km pressure-weighted mean winds. With the study area distantly located between sounding launch sites, R-2 is the best alternative for determining pressure weighted mean winds over the site.

SPATIAL SYNOPTIC CLASSIFICATION

The spatial synoptic classification system (SSC) was originally developed by Larry Kalkstein and Scott Greene (Kalkstein et al. 1996) but was later updated by Scott Sheridan (Sheridan 2002). SSC uses ground-based, station observations measuring properties such as, temperature, wind, pressure, and cloud cover in order to easily classify weather type classifications. By focusing on surface station observations and typifying synoptic behavior rather than trying to parse out the systems' precise origins, SSC allows users to utilize historical observations dating as far back as 1930 while remaining directly comparable to modern day observations. Synoptic weather patterns set the stage for mesoscale and microscale weather occurrences by impacting moisture availability, air temperature, stability, and cyclonic & anti-cyclonic activity.

The SSC dataset is generated using station observations, meaning its resolution is limited to station observations. However, this is hardly an issue as synoptic weather patterns occur on the order of 1,000 km and greater. Further, the resolution of the analysis is limited to one observation per day. SSC classifies observed days into categories of moist or dry, and polar moderate, tropical, or transitional. Together, the combination of these categories describes most, relevant synoptic categorizations such as a humid moist tropical pattern or a frigid dry polar configuration.

METHODS

GAUGE VERIFICATION

Maintenance records were not available for the gauge networks making it necessary to seek alternative methods to verify gauge operability. To ensure functionality of the gauge network, radar imagery was used to verify the presence of meteorological phenomena around the time and within the vicinity of gauge observations. This is performed through the analysis of reflectivity and correlation coefficient radar moments over gauge sites. Reflectivity measures the amount of returned scattering of a radar pulse and may be used to estimate the size and location of scatterers (Rauber and Nesbitt 2016). During a precipitation event, radar pulses are scattered by hydrometers and the reflectivity factor can help to verify the location of hydrometers and the intensity of precipitation. Moderate rainfall is typically understood to produce reflectivity values between 40–50 dBZ while mist to light rain are typically indicated by values less than 40 dBZ. Returns of less than 10 dBZ are typically considered negligible, corresponding to droplets too small to reach the surface.

However, non-meteorological objects, such as swarms of insects, aircraft, and large debris, may also scatter radar beams creating false positive. Therefore, it is also important to estimate the identity of scatterers. A product of dual-pol radar, correlation coefficient can be used to approximate the identity of scatterers by computing the similarity between paired horizontal and vertical radar beams. Meteorological phenomena tend to have high correlation in vertical and horizontal dimensions despite the flattening effect that drag forces have on

rain drops. Accordingly, meteorological phenomena are likely to produce high correlation coefficients, greater than 0.9. Hail and sleet tend to have slightly less correlation typically returning values between 0.85 to 0.95. Non-meteorological phenomena on the other hand typically have very poor horizontal and vertical correlation returning correlation coefficients much less than 0.9.

Utilizing radar reflectivity and correlation coefficient, each gauge observation was analyzed for correspondence with radar imagery. To ensure the availability of imagery, images available from 15 minutes before gauge observations to 10 minutes after were analyzed. Bins were selected that fell within 1 km of a gauge site to leverage potential inaccuracies for gauge locations. Each image was evaluated determining the maximum observed reflectivity and average correlation coefficient at each gauge site. Of each set of images for a given observation, the maximum reflectivity and maximum average correlation coefficient were recorded.

After processing imagery, each gauge's performance was evaluated according to their miss to hit ratio. Misses and hits are defined according to conditions set by skill score tables. The skill score table can be used to analyze the performance of a data set against an alternative dataset. In this case, gauge observations are screened against radar observations. With each observation, radar or gauge observations have the option to indicate either the presence of precipitation or the absence of precipitation. This leads to a total of four possible outcomes when screening the data. The first two possible outcomes indicate that each dataset is in agreeance with the other. In the case that both datasets indicate the presence of precipitation, that observation is recorded as a hit. If neither dataset indicates the presence of rainfall, this may be recorded as a true negative. However, we are most interested in times

when radar and rain gauge observations differ from one another. When an evaluated dataset indicates the presence of rainfall while the control dataset does not, this is considered a missed case by the evaluated dataset, in this case the rain gauge observations. Finally, when the evaluated dataset does not indicate precipitation, but the control dataset does according to our set criteria, this is considered a false positive.

Since the rain gauge data is being evaluated for its performance when making observations, the outcomes being evaluated are hits and misses. Moreover, true negatives would be over representative since we expect it to not be raining most of the time, and false positives are acceptable as we would only expect precipitation a fraction of the time there is observable cloud cover. Therefore, a simple miss to hit ratio is the most effective way to measure gauge performance. By taking the miss to hit ratio, we are able to evaluate the proportion of gauge observations that were not verifiable on radar in relation to the number of observations that are. For the gauge network, rain gauge observations that had at least a maximum reflectivity of 10 dBZ and an average correlation coefficient of 0.9, were considered a successful hit. Those observations that did not meet both of these criteria were flagged as potential misses.

To minimizing the influence of our selected methodology and thresholds, miss to hit ratios at each gauge site were compared to the performance of the rest of the gauge network to create a standard of gauge performance. Therefore, gauges with miss to hit ratios above 1.5 times the inter-quartile range above the 3rd quartile are considered to have extremely poor performance compared to the rest of the network. By using the inter-quartile method we capture typical network behavior while flagging only gauges which were extremely deviant from the rest of the network. Subsequently these gauges were removed from the study.

CALCULATION OF 0–6 KM MEAN WINDS

Storm motion has long been approximated by an average of environmental winds from 0 to 6 km (Bunkers et al. 2000). While it does not take into account dynamical processes that happen within a storm, 0–6 km mean wind is a great way to roughly approximate storm motion in the event of limited available data. To approximate the 0–6 km winds, pressure level reanalysis data was analyzed up to 500 mb, individually for the U (or south to north) and V (or west to east) winds. After calculating vector level pressure weighted mean winds, storm direction over the city can be calculated trigonometrically. 0–6 km mean winds are sufficient to approximate daily wind directions in this study since they will only be used to subset the data temporally. However, future studies should seek more complex means of approximating storm motion.

UPWIND AND DOWNWIND ANALYSIS

To further improve case strength additional parameters were imposed. First, to isolate primarily convective cases, a 40 dBZ minimum threshold was imposed. 40 dBZ has long been recognized as a lower threshold for moderate precipitation. Secondly, in order to properly compare upwind and downwind observations, events were further refined by their maximum network observation. By selecting a threshold of 0.1 inches of rain, the influence of erroneous gauge observations is minimized. Simultaneously, events at the gauges' minimum threshold are eliminated which may appear as large differences between downwind and upwind regions.

Upwind and downwind regions in this study are modeled after previous studies and are defined as regions within +/– 60 degrees of mean wind bearing and within 20 km of the

center of the gauge network. This will provide a small-scale analysis of the regions immediately upwind and downwind of a major urban center. Once upwind and downwind regions are defined, case totals are calculated at each gauge site before being summarized by an areal average in gauges' respective regions. Finally, downwind and upwind regions are compared by calculating the ratio between downwind and upwind areal averages.

Upwind and downwind regions are then analyzed in two ways based on environmental winds. First, events are grouped and summarized based on ordinal directions. In each ordinal direction, events with environmental winds within +/– 45 degrees are selected and evaluated at each gauge site. Upwind and downwind regions are then determined relative to corresponding ordinal directions with upwind being +/– 60 degrees of the selected ordinal direction and downwind defined as +/– 60 degrees of the opposing direction. Afterwards, mean upwind and downwind gauge totals are evaluated before taking the ratio of downwind to upwind total areal average. To determine the significance of observations, the results of each subset are permutated 10,000 times to create a distribution that represents results due to random variation. The significance level is then determined to be the percentage of permutated results that fall above the true observation.

Alternatively, to gain an understanding of upwind and downwind behavior across all cases, looking closely at upwind and downwind regions, the process described above was replicated on a storm by storm basis. This time, rather than using ordinal directions, the evaluated environmental winds per case are used to define upwind and downwind regions. After determining the ratio of downwind to upwind precipitation of each case, the overall upwind to downwind ratio is calculated by taking an average weighted by the maximum rainfall observation of the corresponding event. This process was then also permutated

50,000 to create a random distribution to which to compare the observed downwind to upwind precipitation ratio.

Lastly, to analyze the impact of synoptic conditions, cases were first categorized by synoptic conditions utilizing the SSC database. Total precipitation was then measured at gauge sites for each subset. Additionally, mean wind direction was determined for each subset across the entire study period. Mean wind was utilized to determine upwind and downwind regions relative to the network's center point. Upwind and downwind regions were defined as gauges that fell within 60 degrees of mean winds relative to the network center point. Subsets were then described by taking the ratio of mean downwind to mean upwind precipitation. Lastly, to test for significance, subsets were permutated 10,000 times to create a comparable dataset of randomized behavior. This allows us to estimate the probability of distributions being due to random, natural variation.

RESULTS

GAUGE PERFORMANCE ANALYSIS

The gauge performance analysis was able to identify those gauges which were decommissioned or implemented throughout the study period. This included one gauge, TR17, which took its last observation on July 07, 2018 and four gauges, TR42 through TR46, which were implemented throughout the month of August, 2018. By identifying these gauges, spatial and temporal dimensions can be maximized while maintaining network consistency.

The remaining gauges were then screened for performance. On average, gauges had a ratio of approximately 0.058 misses per hits or 58 misses per 1,000 hits with a standard deviation of 47 misses per 1,000 hits. 50% of the gauges fell between the quantiles of 24 misses per 1,000 hits and 81 misses per 1,000 hits. By taking 1.75 times the inter-quartile range, a threshold value of insufficient accuracy was determined to be at 167 misses per 1,000 hits. Three gauges, TR01, TR20, and TR26, fell above this threshold with miss to hit ratios of 204:1000, 229:1000, and 442:1000 respectively. This reduced the final size of the gauge network to 36 high performing gauges of the total 46.

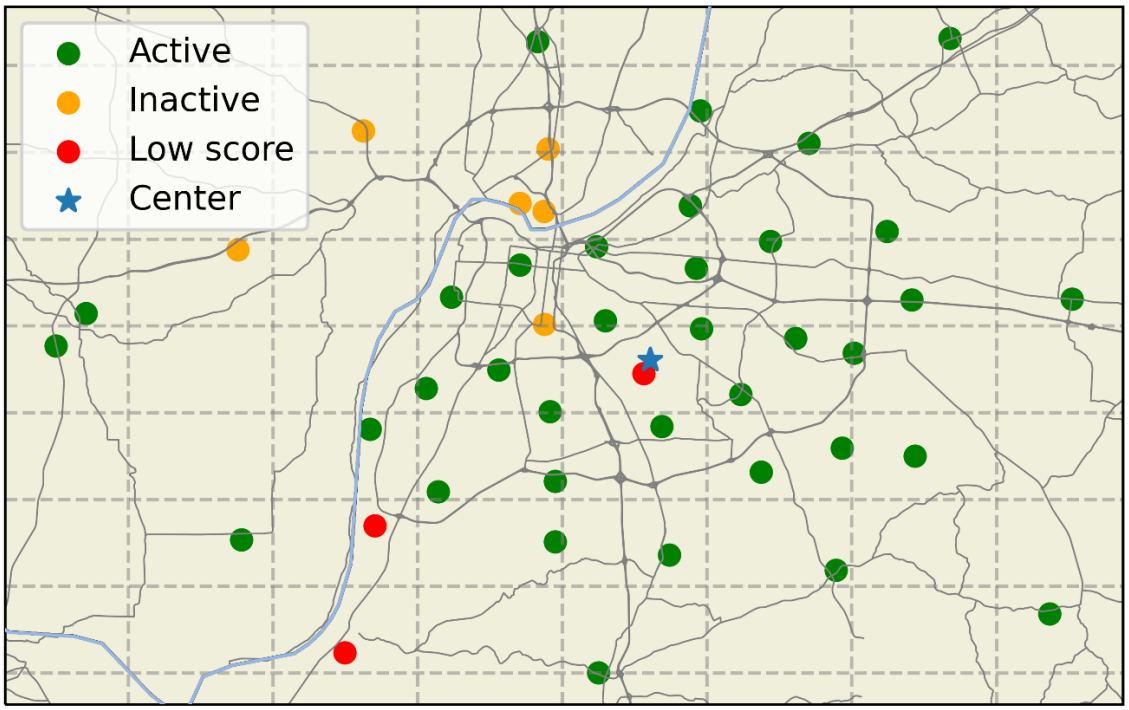

Figure 3. MSD Rain gauge network extent following performance assessment. Active, inactive, and poor performing gauges are displayed as well as the center point of the remaining 36 gauges. Despite 9 gauges being eliminated, the remaining network still provides dense coverage across Louisville, KY and limited coverage across surrounding areas.

Table 1. Results of gauge quality control analysis	
Mean miss:hit ratio	58:1000
Standard deviation	47:1000
1st Quantile	24:1000
3rd Quantile	81:1000
Inter-quartile range	57:1000
Performance threshold	167:1000
Inactive gauges	TR17, TR42, TR43, TR44, TR45, TR46
Poor performing gauges	TR01, TR20, TR26

WARM SEASON, SHORT TERM CLIMATOLOGY (2017-2020)

Warm seasonal winds in Louisville-Jefferson County, KY associated with precipitation come from a bearing of 243 degrees (Figure 4), or southwesterly with average estimated environmental wind speed of 8.5 m/s. Warm season precipitation is on average, 29.5 inches per year (Figure 5). When looking at overall yearly warm season precipitation using mean wind bearing, significant (alpha = 0.05) median downwind enhancement can be observed. Comparing downwind to upwind, gauges downwind experience a median enhancement in precipitation of approximately +9%. Permutating these results 10,000 produced a p-value of .041, showing that there is a strong tendency in Louisville, KY downwind enhancement.

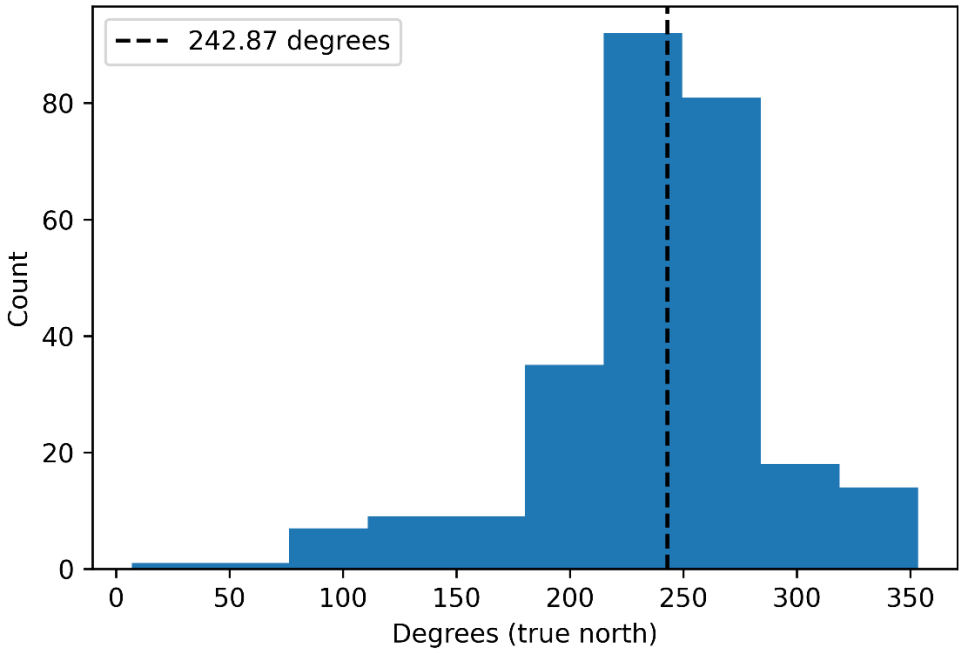

Figure 4. Histogram of mean warm seasonal 0–6 km wind bearings from 2017–2020

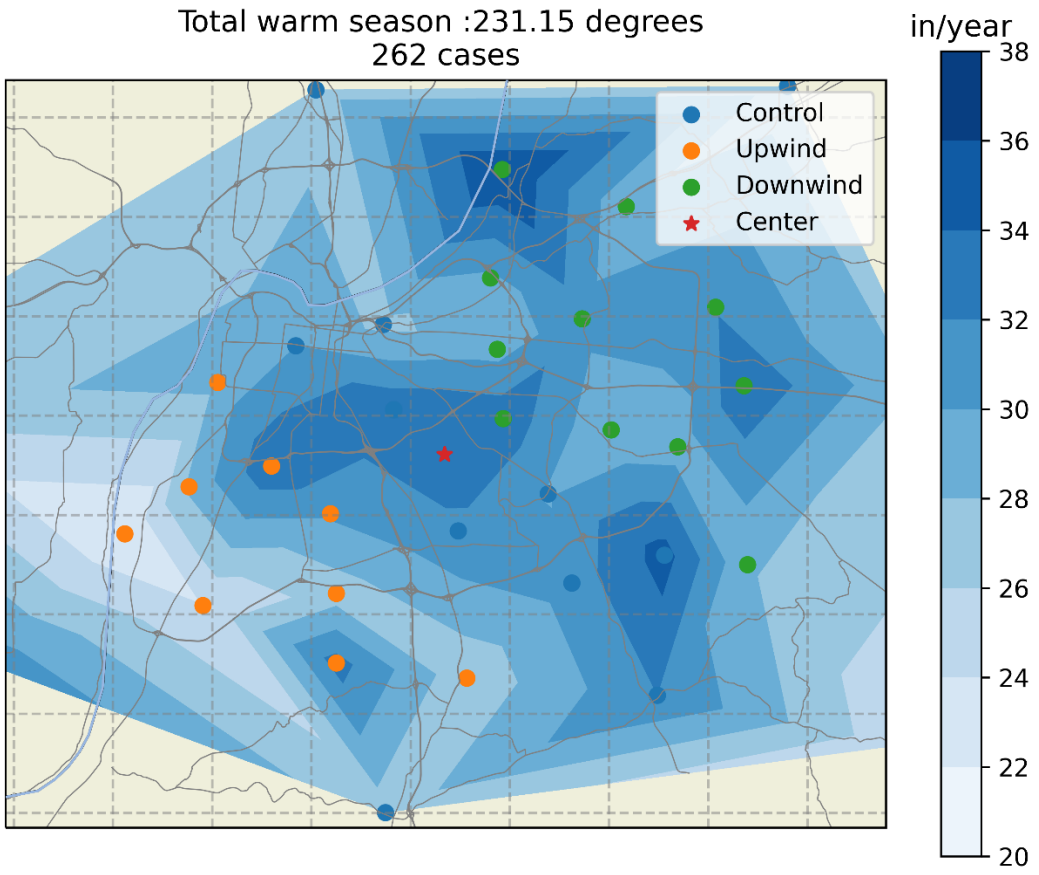

Figure 5. Warm seasonal precipitation 2017–2020 (inches/year).

Warm season precipitation events occur largely under moist tropical synoptic conditions, comprising 53% of significant precipitation events in Louisville (Table 2). This is followed by moist moderate and transitional conditions representing 26% and 11% of warm season precipitation events respectively. However, despite having less than half the number of moist tropical days, moist moderate is responsible for 48% of precipitation while moist tropical is responsible for less than 26% of precipitation. Moist moderate air classifications are diverse in nature, characterizing any synoptic scenarios that cannot clearly be determined to have polar nor tropical qualities according to SSC guidelines. This includes many scenarios along frontal

boundaries such as occluded fronts which did not swiftly transition from one classification to another as well as scenarios where air qualities were mild.

Table 2. Results of upwind–downwind comparison by spatial synoptic classification

SSC class	# of cases	amount (in./year)	mean wind direction	ratio	p-value
Dry moderate	9	0.21”	278	0.91	0.30
Dry polar	1	0.12”	230	1.59	0.004
Dry tropical	4	0.07”	276	5.77	0.0001
Moist moderate	68	14.20”	230	1.10	0.060
Moist polar	14	3.13”	211	0.94	0.19
Moist tropical	73	3.90”	248	1.19	0.010
Transitional	28	4.17”	228	1.13	0.0083
MT +	62	3.69”	233	1.01	0.46
MT ++	3	0.007”	304	2.80	0.59
Total	262	29.50”	231	1.14	0.046

DOWNWIND TO UPWIND ANALYSIS

Table 3 and figure 6 display the results of downwind to upwind comparisons for ordinal subsets. Significant enhancement at 95%–99% confidence was detected in subsets of storm cases with southerly to north westerly flows. Enhancement varied from a +11% to +20% increase in mean precipitation downwind compared to mean observations upwind. This clearly shows that for typical warm season flows, significant downwind enhancement is a dominating pattern.

Table 3. Results of ordinal subset downwind to upwind precipitation ratios

Ordinal wind bearing	range	# of cases	downwind:upwind	p-value
Southerly	145–225	99	1.19	.0016
Southwesterly	180–270	197	1.11	.042
Westerly	225–315	202	1.19	.00090
Northwesterly	270–360	123	1.20	.019
Northerly	315–45	35	1.05	0.37
Northeasterly	0–90	12	0.86	0.17
Easterly	45–135	18	0.98	0.44
Southeasterly	90–180	36	1.09	0.17

Northerly to southeasterly flows however could not display significant and definitive trends in behavior. This is likely in part due to the rarity of such flows. In total, events with environmental winds from directly northwesterly to directly southerly, account altogether for only a total of 50 of 267 cases. Still, northeasterly flows showed a tendency for weak suppression in the downwind region of –14%. While northerly, easterly and southeasterly flows showed only small differences between upwind and downwind regions between – 2% and + 9%.

In the storm by storm analysis, a highly significant median enhancement of +9% was noted between downwind and upwind regions. Results shown in figure 7 show a median ratio of 1.09 or + 9%. This means that the probability that this pattern of downwind enhancement is due to random and natural variation is only 4%. As such, downwind enhancement is the dominant pattern of precipitation across the Louisville MSA.

DOWNWIND TO UPWIND COMPARISON BY SYNOPTIC CLASSIFICATION

Under regular moist tropical and transitional synoptic conditions, statistically significant median downwind enhancement was measured of 20% and 12% respectively (Table 2). Both conditions have a strong southwesterly flow and together account for 27% of yearly warm season precipitation. Statistically significant downwind enhancement was also found under dry polar and dry tropical classifications, however the sample size for these events was very small, averaging less than one precipitable event per year and thus cannot be said to be representative of their corresponding classifications. Notable downwind enhancement was measured in moist moderate with an observed median enhancement and p-value of 9% and .08. This suggests a pattern of downwind enhancement however there is a large amount of ambiguity and diversity associated with moist moderate classifications as

they may represent mild moist polar or tropical conditions as well as slow moving or stationary fronts.

Moist tropical scenarios are further broken down into regular, enhanced, and greatly enhanced moist tropical classifications, named by the SSC as moist tropical, moist tropical plus, and moist tropical double plus. Moist tropical plus scenarios refer to persistently warm days during which both day and night time temperatures are above average while moist tropical double plus refers to moist tropical plus days in which temperatures are at least one standard deviation above mean temperatures. In Louisville, moist tropical and moist tropical plus days are comparable in the number of events and total amount of yearly rainfall. However, the behavior of downwind enhancement is quite different. While in normal moist tropical cases, a strong and statistically significant median downwind enhancement of 20% was measured, moist tropical plus cases measured no significant downwind enhancement with downwind and upwind regions measuring equivalent amounts of precipitation. Moist tropical double plus days in Louisville are rare, accounting for less than 1 case per year.

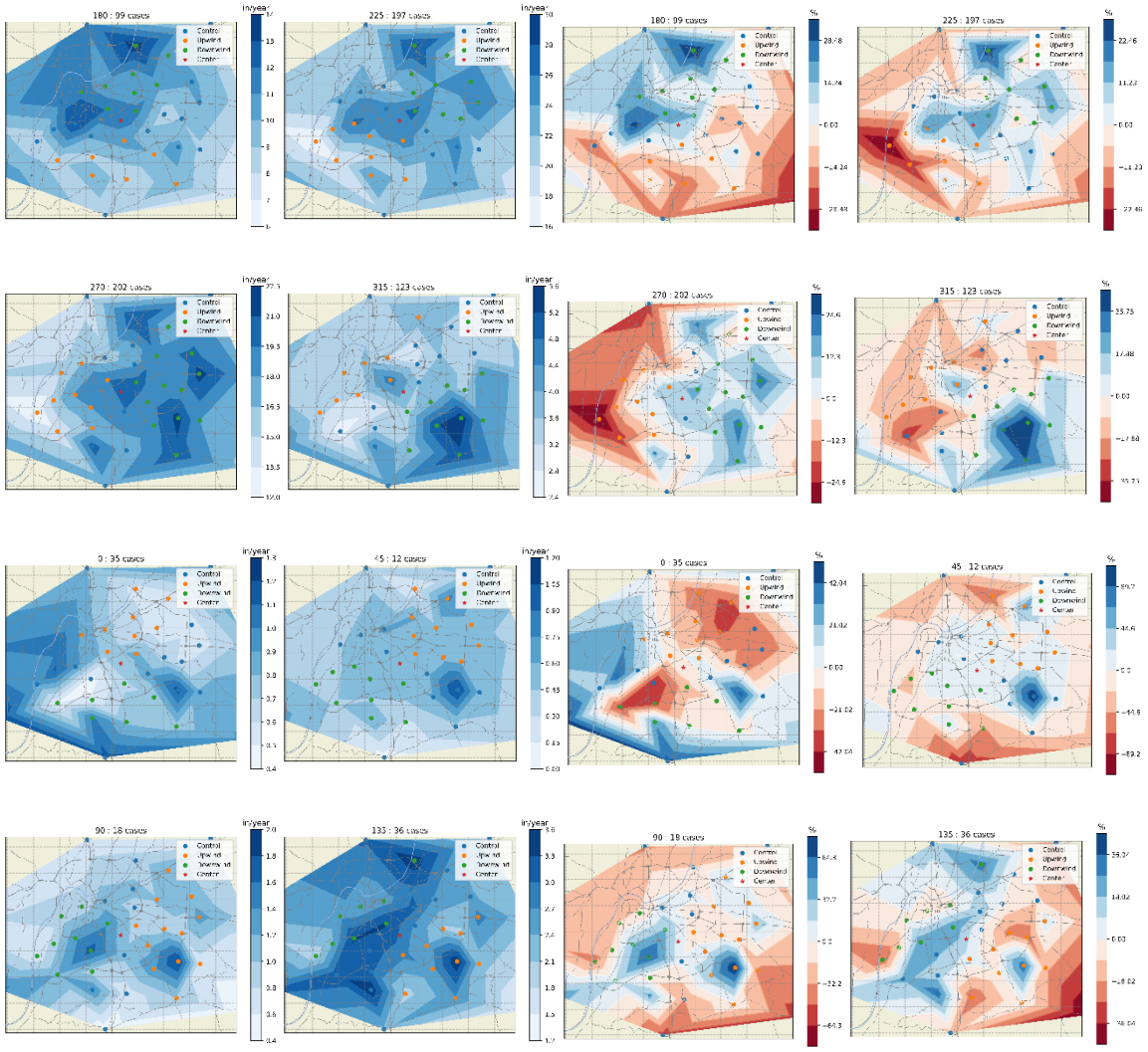

Figure 6. Ordinal directional subsets of (left) total precipitation normalized by mean upwind precipitation and (right) % variance from subset mean precipitation

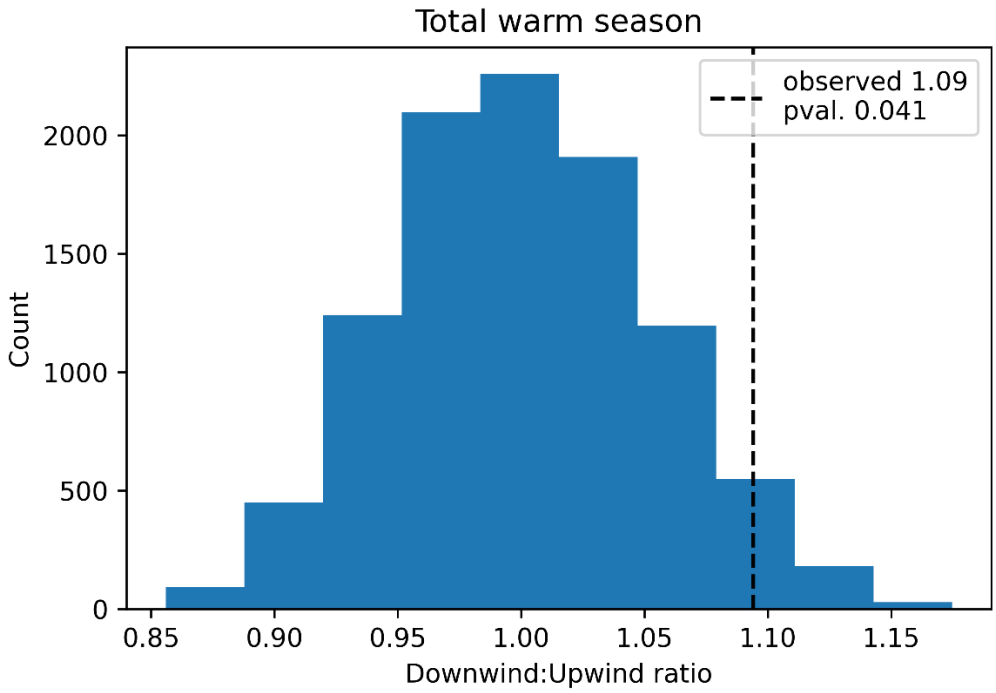

Figure 7. Histogram of the results of permutations of seasonal median downwind to upwind precipitation amounts and the observed median ratio.

CONCLUSIONS

Results of this study show that precipitation across Louisville is dominated by a pattern of downwind enhancement. Median downwind enhancement is shown to be as large as +9% on average when compared to upwind regions, a result highly unlikely to be caused by natural variation in precipitation. It is much more likely tied to changes occurring in precipitable systems as they move across the local area. Although the causes of such enhancement are still largely up to debate.

Synoptic behavior plays a large role in precipitation modification by the urban heat island. As previous studies have reported, urban precipitation modification is strongest under synoptically benign conditions (Dixon and Mote 2003; Bentley et al. 2010). However, significant results under transitional classifications suggests that urban enhancement may also impact more active, frontal classifications. Reduced urban enhancement under moist tropical plus classifications compared to moist tropical classifications suggests that urban enhancement may be driven by differences in surface to air temperatures. Nonetheless, synoptic environments have been shown to be extremely important in the frequency and magnitude of inadvertent urban enhancement.

Despite the prominence of downwind enhancement, inconclusive results associated with the small sample size of atypical flows makes it difficult to pinpoint driving features from this study alone. While the urban environment is the first to raise suspicion, development of the urban environment has occurred in close harmony with the natural

environment. Louisville itself sits within a valley bordered by the Ohio river to the west and north, and elevation increase as large as 100 meters beyond the Ohio as well as to the south. Additionally, the gauge network being owned by a service provider, reflects municipal boundaries rather than being centered around the Louisville MSA which sits at the northeast of municipal boundaries. Even more, intensive industrial and urban land cover change in Louisville has focused heavily on the city's west side, leading to not only an intense heat island effect on the city's west side but increased levels of air pollution as well.

Nonetheless, these confounding variables make Louisville a rich site for urban modification investigations. The organized nature of its downwind precipitation enhancement makes it clear that systems passing over Louisville undergo changes consistent with traditional model of downwind system enhancement even if the processes remain unclear. This research also shows that even with limited maintenance records, publicly available datasets can be vetted using alternative high-resolution datasets such as radar observations. Such a longstanding and growing high density, surface based, dataset could be use in efforts to continue to model Louisville's local environment with increasing accuracy to determine dominant forces of inadvertent precipitation modification.

Future investigations into Louisville's urban precipitation modification should closely consider not just urban development, but the surrounding local environment in which the urban development is entrenched to prove the significance of direct urban forcings, such as the urban heat island effect, in relation to other congruent features such as elevation changes and moisture availability. Through an increased understanding of the many opposing and synergistic characteristics of an urban environment such as Louisville,

so too will our ability to predict and mitigate severe weather at the local scale. As communities downwind of downtown Louisville continue to grow in population and density, more people may be put at risk in the event of urban precipitation enhancement during severe weather. This risk is further exacerbated by the increasing prevalence of extreme weather in a rapidly evolving climate. Therefore, understanding the consequences of urban development and activities as soon as possible, particularly its impact on local weather, is crucial for efficient and effective urban planning.

REFERENCES

68% of the world population projected to live in urban areas by 2050, says UN. 2018. United Nations. https://www.un.org/development/desa/en/news/population/2018-revision-of-world-urbanization-prospects.html.

Bentley, M. L., J. A. Stallins, and W. S. Ashley. 2011. Synoptic Environments favourable for urban convection in Atlanta, Georgia. *International Journal of Climatology* 32 (8):1287–1294.

Bornstein, R., and Q. Lin. 2000. Urban heat islands and summertime convective thunderstorms in Atlanta: Three case studies. *Atmospheric Environment* 34 (3):507–516.

Bunkers, M. J., B. A. Klimowski, J. W. Zeitler, R. L. Thompson, and M. L. Weisman. 2000. Predicting supercell motion using a new hodograph technique. Weather and Forecasting 15 (1):61–79.

Changnon, S.A., R.G. Semonin, and F. A. Huff. 1976. A hypothesis for urban rainfall anomalies. *Journal of Applied Meteorology* 15 (6):544–560.

Debbage, N., and J. M. Shepherd. 2015. The urban heat island effect and city contiguity. Computers, Environment and Urban Systems 54:181–194.

Diem, J., and D. Brown. 2003. Anthropogenic Impacts on Summer Precipitation in Central Arizona, U.S.A. *The Professional Geographer* 55 (3):343-355.

Dixon, P. G., and T. L. Mote. 2003. Patterns and causes of Atlanta's Urban Heat Island–initiated precipitation. *Journal of Applied Meteorology* 42 (9):1273–1284.

Feng, B., Y. Zhang, and R. Bourke. 2021. Urbanization impacts on flood risks based on urban growth data and coupled flood models. Natural Hazards 106 (1):613–627.

Hot Spot Analysis (Getis-Ord Gi*). ArcGIS. https://desktop.arcgis.com/en/arcmap/10.3/tools/spatial-statistics-toolbox/hot-spot-analysis.htm (last accessed 2021).

Huff, F.A., and S.A. Chagnon. 1973. Precipitation Modification by Major Urban Areas. *Bulletin American Meteorological Society* 54 (12):1220-1232.

Kalkstein, L. S., M. C. Nichols, C. D. Barthel, and J. S. Greene. 1996. A new spatial synoptic classification: Application to air-mass analysis. *International Journal of Climatology* 16 (9):983–1004.

Lin, Y., J. Fan, J.-H. Jeong, Y. Zhang, C. R. Homeyer, and J. Wang. 2021. Urbanization-induced land and aerosol impacts on storm propagation and hail characteristics. Journal of the Atmospheric Sciences 78 (3):925–947.

Loose, T., and R.D. Bornstein. 1977. Observations of Mesoscale Effects on Frontal Movement Through an Urban Area. *Monthly Weather Review* 105 (5):563-571.

Louisville MSD Rain Gauge. Louisville MSD. http://raingauge.louisvillemsd.org/ (last accessed 2021).

Matson, M., E. P. Mcclain, D. F. McGinnis, and J. A. Pritchard. 1978. Satellite detection of urban heat islands. Monthly Weather Review 106 (12):1725–1734.

Mölders, N., M. Olson. 2004. Impact of Urban Effects on Precipitation in High Latitudes. *Journal of Hydrometeorology* 5 (3):409-429.

National Land Cover Database 2019 (NLCD2019) statistics for 2019. 2019. National Land Cover Database 2019 (NLCD2019) Statistics for 2019. https://www.mrlc.gov/data/statistics/national-land-cover-database-2019-nlcd2019-statistics-2019.

Naylor, J., and A. Sexton. 2018. The relationship between severe weather warnings, storm reports, and storm cell frequency in and around several large metropolitan areas. *Weather and Forecasting* 33 (5):1339–1358.

Naylor, J. 2020. Idealized simulations of city-storm interactions in a two-dimensional framework. *Atmosphere* 11 (7):707.

Next generation weather radar. 2021. National Centers for Environmental Information (NCEI). https://www.ncei.noaa.gov/products/radar/next-generation-weather-radar.

Ochs, H., and R.G. Semonin. 1979. Sensitivity of a Cloud Microphysical Model to an Urban Environment. *Journal of Applied Meteorology* 18:1118-1129.

PRB's 2021 World Population Data Sheet. 2021. Population Reference Bureau. https://interactives.prb.org/2021-wpds/.

Rauber, R. M., and S. W. Nesbitt. 2016. Dual-polarization radar. In Radar meteorology: A first course, 126–176. John Wiley & Sons.

Rosenfeld, D. 2000. Suppression of rain and snow by urban and Industrial Air Pollution. Science 287 (5459):1793–1796.

Shepherd, J.M. 2002. Rainfall Modification using Spaceborn Radar TRMM. *Journal of Applied Meteorology and Climatology* 41 (7):689-701.

Shepherd, J.M. 2005. A review of current investigations of urban-induced rainfall and recommendations for the future. *Earth Interactions* 9 (12):1–27.

Shepherd, J.M., and S.J. Burian. 2003. Detection of urban-induced rainfall anomalies in a major coastal city. *Earth Interactions* 7 (4):1–17.

Sheridan, S. C. 2002. The redevelopment of a weather-type classification scheme for North America. *International Journal of Climatology* 22 (1):51–68.

Stone, B. 2007. Urban and rural temperature trends in proximity to large US cities: 1951–2000. International Journal of Climatology 27 (13):1801–1807.

Thielen, J., W. Wobrock, A. Gadian, P.G. Mestayer, and J.D. Cruetin. 2000. The possible influence of urban surfaces on rainfall development: a sensitivity study in 2D in the meso-gamma-scale. *Atmospheric Research* 54:15-39.

TRMM instruments. 2022. Global Precipitation Measurement. https://gpm.nasa.gov/missions/TRMM/satellite.

World urbanization prospects country profiles. 2018. United Nations Department of Economic and Social Affairs. https://population.un.org/wup/Country-Profiles/.

CURRICULUM VITA

NAME: Isaiah Ishmaiah Kingsberry

ADDRESS: Department of Geography & Environmental Sciences
2301 S. Third St.
University of Louisville
Louisville, KY 40292

DOB: Tacoma, Washington - May 01, 1996

EDUCATION
& TRAINING: B.S., Atmospheric Science
University of Louisville
2014 – 2018

M.S., Applied Geography
University of Louisville
2020 – Expected 2022

AWARDS: Carol Hanchette Award for Outstanding Graduate Student
2022

PROFESSIONAL SOCIETIES: American Meteorological Society
2021 – Current

American Geophysical Union
2020 – 2021